Makara Journal of Science

Volume 25
Issue 4 *December*

Article 2

12-30-2021

Effect of Dry Oxidation and Thermal Annealing on AlN/GaN/AlN/Si (111) and Evaluation of its Electrical Characteristics

Mohd Zaki Mohd Yusoff
Department of Applied Sciences, Universiti Teknologi MARA, Cawangan Pulau Pinang, Permatang Pauh 13500, Malaysia, zaki7231@uitm.edu.my

Azzafeerah Mahyuddin
Universiti Kuala Lumpur, Malaysian Institute of Industrial Technology (MITEC), Bandar Seri Alam, Johor 81750, Malaysia

Zainuriah Hasssan
Institute of Nano-Optoelectronics Research and Technology, Universiti Sains Malaysia, Penang 11800, Malaysia

Muhammad Syarifuddin Yahya
Faculty of Ocean Engineering Technology and Informatics, Universiti Malaysia Terengganu, Kuala Nerus 21030, Terengganu, Malaysia

Recommended Citation

Mohd Yusoff, Mohd Zaki; Mahyuddin, Azzafeerah; Hasssan, Zainuriah; and Yahya, Muhammad Syarifuddin (2021) "Effect of Dry Oxidation and Thermal Annealing on AlN/GaN/AlN/Si (111) and Evaluation of its Electrical Characteristics," *Makara Journal of Science*: Vol. 25 : Iss. 4 , Article 2.
DOI: 10.7454/mss.v25i4.1249
Available at: https://scholarhub.ui.ac.id/science/vol25/iss4/2

Makara Journal of Science, 25/4 (2021), 203–209
doi: 10.7454/mss.v25i4.1249

Effect of Dry Oxidation and Thermal Annealing on AlN/GaN/AlN/Si (111) and Evaluation of its Electrical Characteristics

Mohd Zaki Mohd Yusoff[1*], Azzafeerah Mahyuddin[2], Zainuriah Hassan[3], and Muhammad Syariffudin Yahya[4]

1. Department of Applied Sciences, Universiti Teknologi MARA, Cawangan Pulau Pinang, Permatang Pauh 13500, Malaysia
2. Universiti Kuala Lumpur, Malaysian Institute of Industrial Technology (MITEC), Bandar Seri Alam, Johor 81750, Malaysia
3. Institute of Nano-Optoelectronics Research and Technology, Universiti Sains Malaysia, Penang 11800, Malaysia
4. Faculty of Ocean Engineering Technology and Informatics, Universiti Malaysia Terengganu, Kuala Nerus 21030, Terengganu, Malaysia

E-mail: zaki7231@uitm.edu.my

Received June 12, 2021 | Accepted September 27, 2021

Abstract

We proposed a technique for improving the platinum (Pt) Schottky contact dark current of the AlN/GaN/AlN/Si(111) substrate. The AlN/GaN/AlN/ heterostructure sample was successfully grown on a silicon substrate by radio frequency molecular beam epitaxy. The high quality of the interlayer heterostructure sample was verified by transmission electron microscopy (TEM). From the TEM image, a good quality single interface layer with spacing less than 1 nm was detected. The strong significant peaks obtained by X-ray diffraction measurement indicated that the sample has a high structural quality for each grown layer. Dry oxidation and thermal annealing were used in conjunction to effectively reduce the leakage current of the Schottky contact of the AlN/GaN/AlN/Si(111) substrate. Energy-dispersive X-ray analysis revealed the presence of the element oxygen. Dry oxidation enhanced the surface roughness and surface-active area of the samples. Al_2O_3 contributed to the low leakage current of the Pt Schottky contact of the AlN/GaN/AlN/Si(111) substrate. The Al_2O_3 layer acted as an insulator layer, and retarded the current flow of devices.

Keywords: aluminum nitride, annealing, oxidation mechanism, silicon substrate, thermal oxidation

Introduction

III-nitride semiconductor device development has a significant impact on a variety of technologies, including information storage, full color displays, true color copying, underwater communications, local area networks, space-to-space communications, high temperature power electronics, and microwave electronics [1–3]. The use of aluminum nitride (AlN) as a buffer layer for the development of device grade gallium nitride (GaN), as well as for applications in electroacoustic, acousto-optic, and optoelectronic devices, has particularly drawn substantial attention [4]. The high thermal conductivity (82–170 W/mK), high density, broad bandgap, and high electrical resistance of ceramic AlN material make it particularly popular in the electronic industries, particularly for applications in thermally conductive devices [5]. Because it enables in-situ measurement of surface roughness and rebuilding during growth, molecular beam epitaxy (MBE) is an excellent technology for device development. Silicon substrates provide well-known technological benefits, are inexpensive, and can be used for hybrid integration. Schottky contact is the preferred metal contact type for metal–semiconductor–metal photodetectors because of their low dark current and good performance [6]. The high quality of the crystal structure and the high value of the Schottky barrier height (SBH) are the main factors in achieving a good rectifying behavior of Schottky contact. The low leakage current of the Schottky contact contributes to the high ratio of photocurrent to dark current, subsequently reducing the consumption of operating power. To achieve a low dark current on a device, we can use high work function metals. However, many high-work-function metals are unstable. Moreover, at the metal–AlN interface, considerable interdiffusion could occur. The formation of an oxide layer between the metal and the AlN layer is believed to solve the interdiffusion problem and suppress the dark current of the photodetectors. Thermal treatment is normally used to improve the metal deposition contact or enhance the structural quality of the as-grown layers. Furthermore, thermal treatment

is used to oxidize the AlN film at a certain high temperature.

The AlN film tends to form an oxide layer, which consists of aluminium oxide (Al_2O_3), when sufficient temperature and time are provided during the thermal oxidation process. A thin oxide layer is grown between the contact and the semiconductor through the oxidation process to successfully lower the reverse leakage current of the device. Thermal oxidation process is also an effective method to increase the size of the surface active area. However, thermal treatment can reduce the capability of AlN to a good thermal conductivity [7]. Generally, AlN powder is oxidized at temperatures of 550 °C–1,100 °C [8]. Oxidation treatment of thin films have been reported by other researchers at temperatures ranging from 1,000 ºC to 1,390 ºC [8]. Studies on the effect of the oxidation process on AlN powder [8] and bulk [9–14] have been conducted by many researchers.

To the best of our knowledge, no reports on the effect of oxidation on high quality AlN layers have been published. The AlN/GaN/AlN heterostructure layers were grown on silicon substrate by radio frequency MBE (RF-MBE). The AlN/GaN/AlN/Si substrate is beneficial to the fabrication of high reliability metal–oxide–semiconductor field-effect transistor and metal-oxide-semiconductor capacitor devices. Moreover, the effect of thermal annealing of platinum (Pt)-oxidized AlN/GaN/AlN on Si substrate was investigated. On this basis, the relationship between the thermal annealing on Pt-oxidized samples at different temperatures was discussed, which includes ideality factor and Schottky barrier height values to the sample.

In this work, dry oxidation treatment was used to form Al_2O_3 on the AlN/GaN/AlN/Si(111) substrate. The surface morphological, structural, and electrical properties of the samples are investigated by scanning electron microscopy (SEM), atomic force microscopy (AFM), high-resolution X-ray diffraction (HR-XRD), and current–voltage (*I–V*) source meter. The transformation of the surface of the sample before and after oxidation is investigated in detail. Energy-dispersive X-ray (EDX) analysis confirmed the presence of the element oxygen that emerges from the Al_2O_3 surface layer after the dry oxidation process was completed. The AFM measurement showed that the oxidized sample has a rougher surface than the control sample because of the formation of the oxide layer, which consists of Al_2O_3, on the surface of the sample.

Methods

A Veeco RF-MBE machine is used to grow the AlN/GaN/AlN/Si(111) substrates. To analyze the effects of dry oxidation and thermal annealing on the sample,

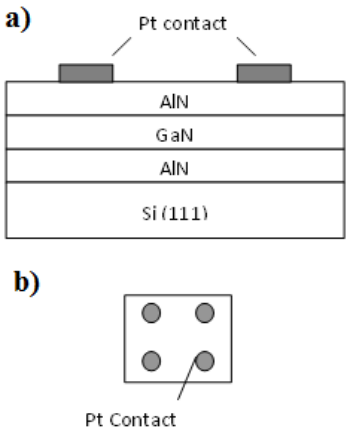

Figure 1. (a) Cross-sectional and (b) Top Views of the Schematic Design of Pt Schottky Contact Fabricated on the Sample

the sample is placed in a conventional tube furnace in dry oxygen ambient for 75 min. The cross-sectional image of the AlN/GaN/AlN/Si(111) sample was examined by transmission electron microscopy (TEM; Model: JEOL). The surface morphology and composition of each element of the sample were analyzed by field-emission SEM (Model: FEI Nova NanoSEM 450) and Energy EDX, (Model: FEI Nova NanoSEM 450), respectively. The surface roughness and structural property of the samples were determined by AFM (Model: Dimension EDGE, BRUKER) and HR-XRD, (Model: PANalytical X'Pert PRO MRD PW3040), respectively. The metal mask used for Schottky contact fabrication consists of an array of dots with a diameter of 200 µm. The Pt contacts were placed on the top surface of the samples (see Figures 1(a) and 1(b)). A radio frequency sputtering machine (Model: Auto HHV500) was used to fabricate Pt contacts on the samples. Then, the fabricated Pt Schottky diodes were annealed for 10 min at temperatures of 500 °C and 700 °C in a conventional tube furnace in a flowing nitrogen environment. The electrical properties of the Schottky diodes were (analyzed based on the current-voltage the *I–V*) characteristics of the device. The Keithley Model 82 simultaneous C–V system was used to measure the *I–V* characteristics of the device.

Results and Discussion

TEM images of the interface between three nitride layers and the silicon substrate were obtained (refer to Figure 2). A clear thin layer was observed for each nitride layer with a thickness of 69.94, 345.3, and 103.4 nm for the AlN, GaN, and AlN buffer layers, respectively. Notably, the interface layers contained defects with a disordered arrangement because of the occurrence of lattice mismatch between layers. Figure 3 shows the SEM images of the (a) control and (b) oxidized samples. The oxidized sample has a higher surface roughness than the

control sample. More oxide pores formed at the surface layer because of the interchange between the elements nitrogen and oxygen. The AlN layer is transformed into oxide form in the temperature range of 800 °C to 900 °C and completely transformed to the oxide layer at 1,100°C for 3 h [11]. The oxidation of AlN induces metalization because the surface-active area is larger than the actual adhesion area [14, 15]. Lee et al. [11] reported the nucleation of three-dimensional (3-D) islands, as well as triangular and circular islands, on the AlN surface when the oxidation temperature reaches 800 °C.

Figure 4 shows the AFM images of the (a) two-dimensional (2D) and (b) 3D control samples and (c) 2D and (d) 3D oxidized samples. The root–mean–square (RMS) value of the control sample is 0.0544 µm, whereas the RMS value of the oxidized sample is 0.547 µm. The results are consistent with the SEM images. The oxidized sample has a rougher surface than the control sample because of the formation of the oxide layer during the oxidation process. With sufficient temperature, the oxygen ion can easily replace the nitrogen ion during AlN bonding to form Al_2O_3. Cao et al. (2017) detected large pores on the oxide surface after annealing the AlN powder at temperatures between 900 °C and 1,300 °C in ambient air [16]. The formed oxide surface is believed to become granular or bubble-like when the sample is annealed in dry oxygen ambient [17]. Meanwhile, the structure of the oxide surface becomes semicrystalline columnar when the AlN layer is annealed in mixed wet and dry oxygen ambient [18]. Yeh et al. (2017) revealed that the grown oxide surface of polycrystalline AlN is not continuous after annealing the sample under dry air conditions at a temperature of 1,150 °C [19]. The oxide surface of AlN powder has pores and cracks [20] and becomes more porous [21] after annealing in ambient air and dry oxygen ambient, respectively. Meanwhile, the oxide layer grown on single-crystalline AlN in dry oxygen ambient is believed to have amorphous characteristics [22].

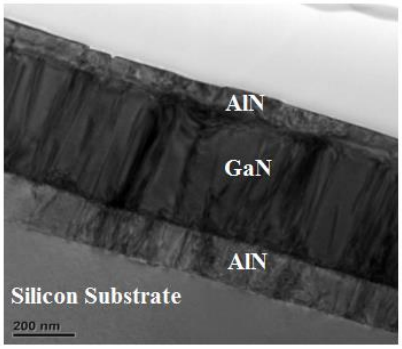

Figure 2. TEM Image of the Control Sample

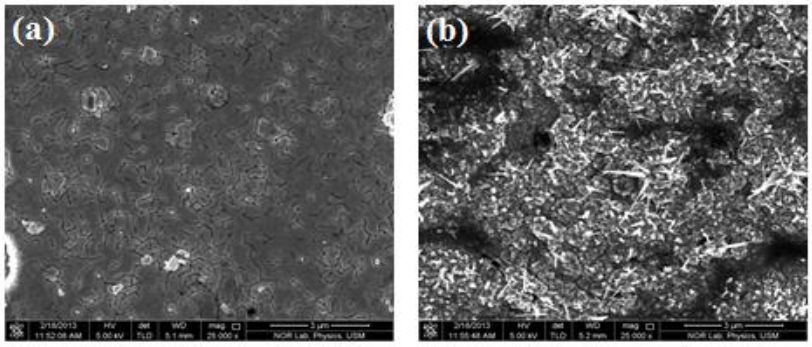

Figure 3. SEM Images of the (a) Control and (b) Oxidized Samples

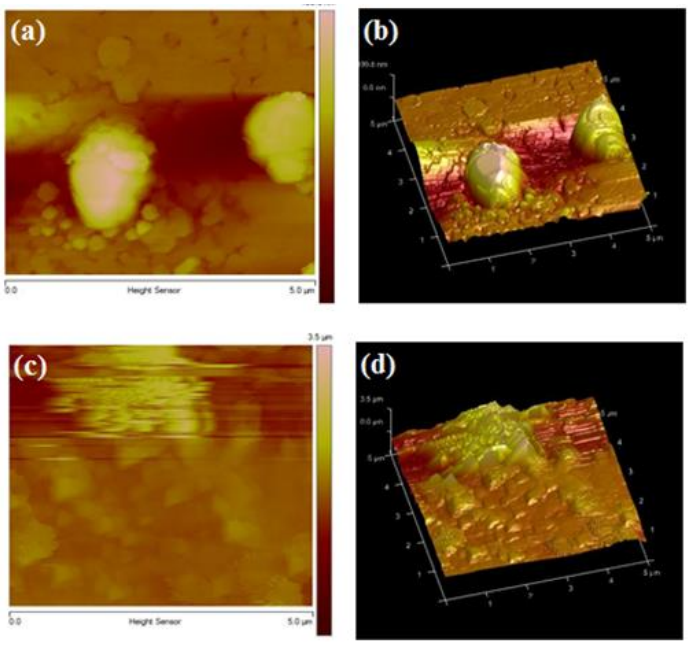

Figure 4. AFM Images of the (a) 2D and (b) 3D Control Samples and (c) 2D and (d) 3D Oxidized Samples

Figure 5 shows the EDX analysis of the samples. All of the samples were free of any contamination or foreign elements. Notably, the oxidized sample contained the element oxygen (see Figure 5(b)). EDX analysis confirmed the presence of Al_2O_3 at 21.29 wt% on the surface of the sample. Figure 6 shows the XRD scans for the control and oxidized samples. The presence of AlN/GaN/AlN layers on the samples was validated by the XRD spectra. The XRD spectra of the samples do not show any oxide phase, indicating that the oxide layer is thinner than all of the grown layers. Figure 7 shows the *I–V* characteristics of the oxidized sample under dark conditions, operating under forward and reverse biases. The electrical characteristics of the Pt Schottky contact show the rectifying behavior. The inset graph shown in Figure 7 indicates the replotted data for the oxidized sample. All of the *I–V* results show the Schottky behavior. The oxidized samples show lower current responses than the control samples.

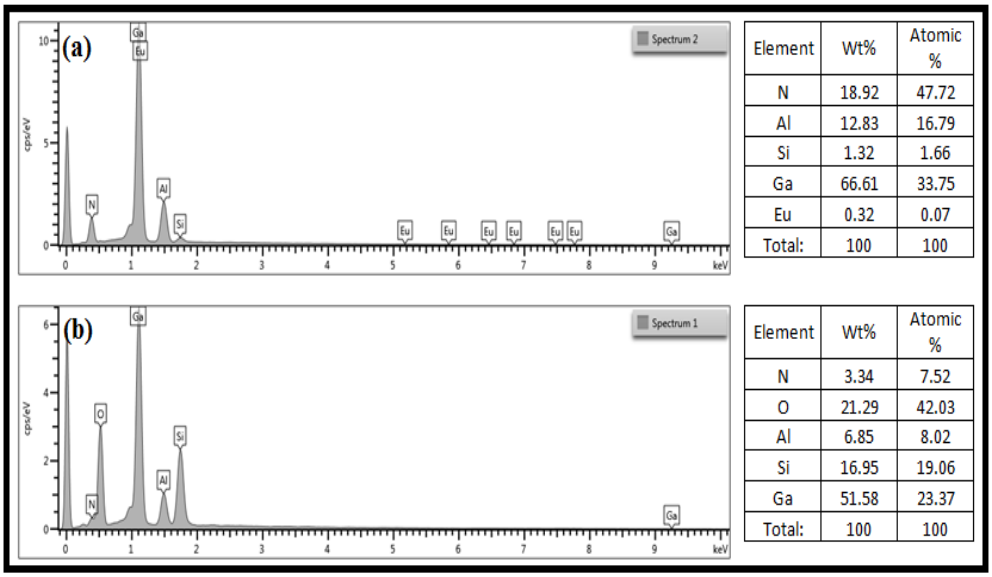

Element	Wt%	Atomic %
N	18.92	47.72
Al	12.83	16.79
Si	1.32	1.66
Ga	66.61	33.75
Eu	0.32	0.07
Total:	100	100

Element	Wt%	Atomic %
N	3.34	7.52
O	21.29	42.03
Al	6.85	8.02
Si	16.95	19.06
Ga	51.58	23.37
Total:	100	100

Figure 5. EDX Analysis of the (a) Control and (b) Oxidized Samples

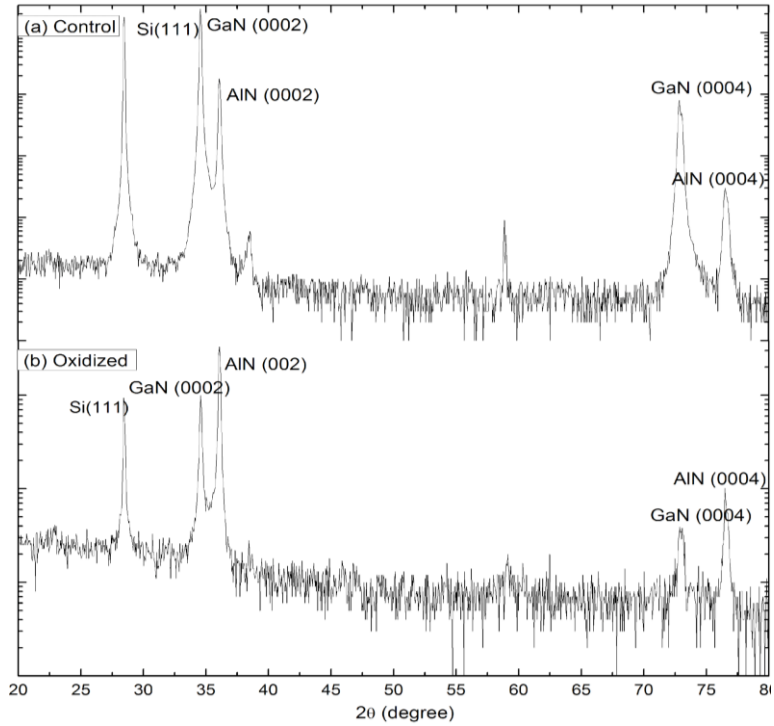

Figure 6. XRD Analysis of the (a) Control and (b) Oxidized Samples

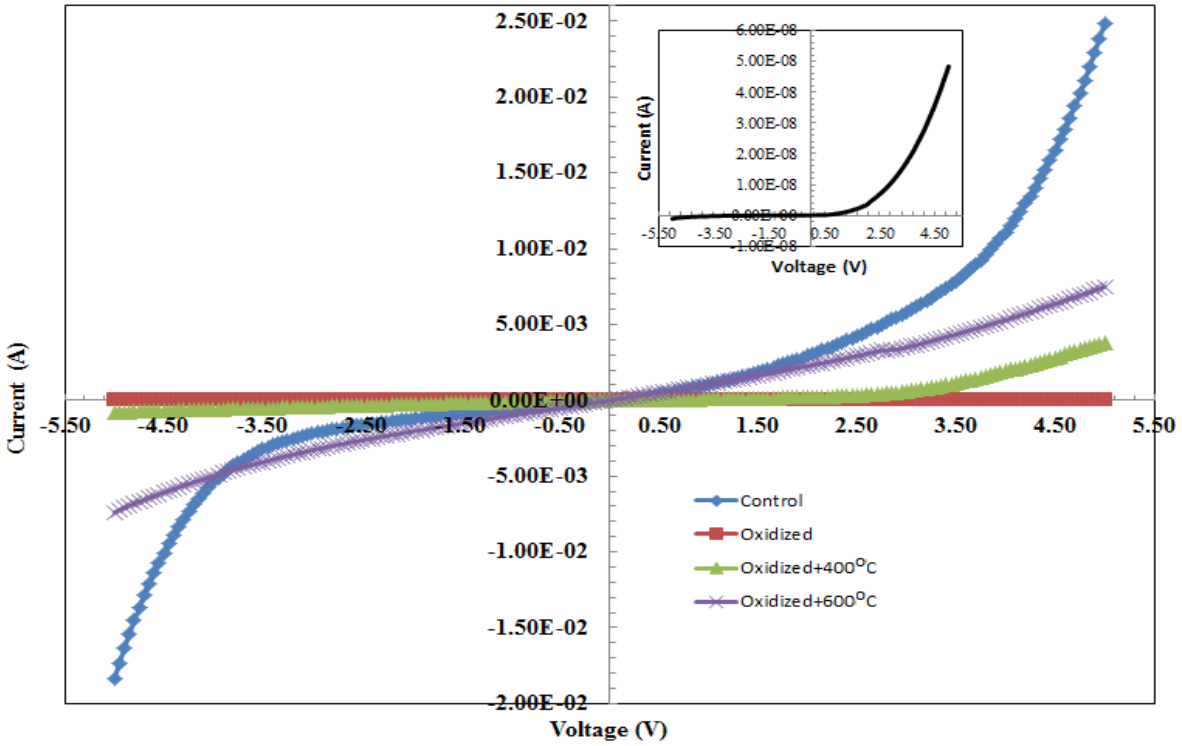

Figure 7. Electrical Characteristics of Schottky Contact on the Oxidized Sample

The grown oxide layer acted as an insulated layer and retarded the electron flow, subsequently contributing to the low current flow. Moreover, because of the difference in the coefficient of thermal expansion between AlN (4.5×10^{-6}°C^{-1}) and Al_2O_3 (8.8×10^{-6}°C^{-1}) [15], mismatched structures are believed to form at the AlN–Al_2O_3 interface during the cooling process. The oxidized samples annealed at 400 °C and 600 °C have higher current responses than the oxidized sample without thermal annealing.

The detailed analysis of the Schottky contact property of the Pt-dotted contacts can be well investigated using the following equation [23,24]:

$$I = I_o \exp\left(eV/nKT\right)\left[1 - \exp\left(-eV/kT\right)\right] \quad (1.0)$$

where I is the obtained current, I_o is the saturated current, V is the applied voltage, and n is the ideality factor. I_o can be expressed as follows:

$$I_o = SA^*T^2 \exp\left(-q\Phi_B / kT\right) \quad (2.0)$$

where S is the active area, Φ_B is the SBH, and A^* is the Richardson parameter. Equation (1.0) can also be expressed as follows:

$$\frac{I \exp(eV/kT)}{\exp(eV/kT) - 1} = I_0 \exp(eV/nkT) \quad (3.0)$$

When temperature $T \leq 370$ K and the applied voltage $V \leq -0.5$ V, Equation (3.0) can be rewritten as follows:

$$I \exp(\frac{eV}{kT}) = I_0 \exp(\frac{eV}{nkT}) \quad (4.0)$$

$$\ln I + \frac{eV}{kT} = \ln I_o + \frac{eV}{nkT} \quad (5.0)$$

Finally, the plot of $\left(\ln I + \frac{eV}{kT}\right)$ vs. V will yield a straight line of the slope $= e/nkT$ and y-intercept at $\ln I_o$.

Table 1 shows the summary of the electrical characteristics of the samples. Generally, we determined that dry oxidation treatment resulted in more significant changes to the SBH of the oxidized sample than the control sample. Dry oxidation and thermal annealing have

Table 1. SBH and Ideality Factor of the Samples

Sample	Ideality actor, *n*	Barrier height, Φ_B (eV)	Current at 5 V (μA)
Control	1.02	0.391	24,884.63
Oxidized	1.03	0.837	0.04
Oxidized + 400°C	1.02	0.430	3,810.32
Oxidized + 600°C	1.02	0.371	747.90

increased the barrier height and decreased the current value. The stabilities of the ideality factor for all of the samples indicate that dry oxidation does not affect the metal contact interface. If the ideality factor value is higher than 1, then series resistance dominates the current slope in the forward current. The high ideality factor value can be attributed to the barrier inhomogeneities, interfacial oxide layers, and series resistance under forward bias conditions [25].

Conclusion

We have successfully demonstrated a simple method to modify the leakage current of the Pt Schottky contact of the AlN/GaN/AlN/Si(111) sample using dry oxidation treatment. The sample was grown by RF-MBE on a silicon substrate. The high morphological and structural qualities of the samples were confirmed using the TEM and XRD machines. The presence of the element oxygen is confirmed by EDX measurement. The dry oxidation process is believed to increase the surface roughness of the samples. Consequently, the Al_2O_3 layer is believed to produce a low leakage current. Finally, the SBH is determined to have a lower value after the formation of Al_2O_3.

Acknowledgements

This work was conducted under the research university grant 1001/PFIZIK/814189. The support from Universiti Sains Malaysia and Universiti Teknologi MARA is gratefully acknowledged.

References

[1] Beladjal, K., Kadri, A., Zitouni, K., Mimouni, K. 2021. Bandgap bowing parameters of III-nitrides semiconductors alloys. Superlattice. Microst. 155: 106901, https://doi.org/10.1016/j.spmi.2021.106901.

[2] Chen, F., Ji, X., Lau, S.P. 2020. Recent progress in group III-nitride nanostructures: From materials to applications. Mater. Sci. Eng. Rep. 142: 100578, https://doi.org/10.1016/j.mser.2020.100578.

[3] Yu, J., Hao, Z., Deng, J., Yu, W., Wang, L., Luo, Y., Wang, J., Sun, C., Han, Y., Xiong, B., Li, H. 2020. Influence of nitridation on III-nitride films grown on graphene/quartz substrates by plasma-assisted molecular beam epitaxy. J. Crystal Growth. 547: 125805, https://doi.org/10.1016/j.jcrysgro. 2020.125805.

[4] Morkoç, H., Di Carlo, A., Cingolani, R. 2002. GaN-based modulation doped FETs and UV detectors. Solid-State Electr. 46(2): 157–202, https://doi.org/10.1016/S0038-1101(01)00271-4.

[5] Whiteside, M., Arulkumaran, S., Dikme, Y., Sandupatla, A., Ng, G.I. 2020. Improved interface state density by low temperature epitaxy grown AlN for AlGaN/GaN metal-insulator-semiconductor diodes. Mater. Sci. Eng. B. 262: 114707, https://doi.org/10.1016/j.mseb.2020.114707

[6] Mohammadnejad, S., Maklavani, S.E., Rahimi, E. 2008. Dark current reduction in ZnO-based MSM photodetectors with interfacial thin oxide layer. In 2008 International Symposium on High Capacity Optical Networks and Enabling Technologies, IEEE. pp. 259–264.

[7] Yeh, C.T., Tuan, W.H. 2015. Pre-oxidation of AlN substrates for subsequent metallization. J. Mater. Sci. Mater. Electr. 26(8): 5910–5916, https://doi.org/10.1007/s10854-015-3160-7.

[8] Yeh, C.T., Tuan, W.H. 2017. Oxidation mechanism of aluminum nitride revisited. J. Adva. Ceram. 6(1): 27–32, https://doi.org/10.1007/s40145-016-0213-1.

[9] Korbutowicz, R., Zakrzewski, A., Rac-Rumijowska, O., Stafiniak, A., Vincze, A. 2017. Oxidation rates of aluminium nitride thin films: effect of composition of the atmosphere. J. Mater. Sci. Mater. Electr. 28(18): 13937–13949, https://doi.org/10.1007/s10854-017-7243-5.

[10] Kim, H.E., Moorhead, J.A. 1994. Oxidation behavior and flexural strength of aluminum nitride exposed to air at elevated temperatures. J. Am. Ceram. Soc. 77(4): 1037–1041, https://doi.org/10.1111/j.1151-2916.1994.tb07264.x.

[11] Lee, J.W., Radu, I., Alexe, M., 2002. Oxidation behavior of AlN substrate at low temperature. J. Mater. Sci. Mater. Electr. 13(3): 131–137, https://doi.org/10.1023/A:1014377132233.

[12] Geng, Y., Norton, M.G. 1999. Early stages of oxidation of aluminum nitride. J. Mater. Res. 14(7): 2708–2711, https://doi.org/10.1557/JMR.1999.0363.

[13] Sato, T., Haryu, K., Endo, T., Shimada, M. 1987. High temperature oxidation of hot-pressed aluminium nitride by water vapour. J. Mater. Res. 22(6): 2277–2280, https://doi.org/10.1007/BF01132972.

[14] Bellosi, A., Landi, E., Tampieri, A. 1993. Oxidation behavior of aluminum nitride. J. Mater. Res. 8(3): 565–572, https://doi.org/10.1557/ JMR.1993.0565.

[15] Osborne, E.W., Norton, M.G. 1999. Oxidation of aluminium nitride. Journal of materials science, 33(15): 3859–3865, https://doi.org/10.1023/A:1004667906474.

[16] Cao, C., Feng, Y., Qiu, T., Yang, J., Li, X., Liang, T., Li, J. 2017. Effects of isothermal annealing on the oxidation behavior, mechanical and thermal properties of AlN ceramics. Ceram. Int. 43(12): 9334–9342, https://doi.org/10.1016/j.ceramint.2017.04.098.

[17] Placidi, M., Perez-Tomas, A., Moreno, J.C., Frayssinet, E., Semond, F., Constant, A., Godignon, P., Mestres, N., Crespi, A., Millan, J. 2010. Interfacial properties of AlN and oxidized AlN on Si. Surf. Sci. 604(1): 63–67, https://doi.org/10.1016/j.susc.2009.10.022.

[18] Domanowska, A., Korbutowicz, R., Teterycz, H. 2019. Morphology and element composition profiles of alumina films obtained by mixed thermal oxidation of AlN epitaxial layers. Appl. Surf. Sci. 484: 1234–1243, https://doi.org/10.1016/j.apsusc.20 19.03.319.

[19] Yeh, C.T., Tuan, W.H. 2017. Accelerating the oxidation rate of AlN substrate through the addition of water vapor. J. Asian Ceram. Soc. 5(4): 381–384, https://doi.org/10.1016/j.jascer.2017.08.001.

[20] Jiang, H., Wang, X.H., Fan, G.F., Fu, M., Lei, W., Wang, X.C., Liang, F., Lu, W.Z. 2019. Effect of oxidation on flexural strength and thermal properties of AlN ceramics with residual stress and impedance spectroscopy analysis of defects and impurities. Ceram. Int. 45(10): 13019–13023, https://doi.org/10.1016/j.ceramint.2019.03.232.

[21] Hou, X., Chou, K.C., Zhong, X., Seetharaman, S. 2008. Oxidation kinetics of aluminum nitride at different oxidizing atmosphere. J. Alloys Compounds. 465(1–2): 90–96, https://doi.org/10.1016/j.jallcom.2007.10.066.

[22] Chaudhuri, J., Nyakiti, L., Lee, R.G., Gu, Z., Edgar, J.H., Wen, J.G. 2007. Thermal oxidation of single crystalline aluminum nitride. Mater. Characterization. 58(8–9): 672–679, https://doi.org/10.1016/j.matchar.2006.11.013.

[23] Rhoderick, E.H. 1982. Metal-semiconductor contacts. IEE Proc. I-Solid-State Electr. Devic. 129(1): 1, https://doi.org/10.1049/ip-i-1.1982.0001.

[24] Rideout, V.L. 1975. A review of the theory and technology for ohmic contacts to group III–V compound semiconductors. Solid State Electr. 18(6): 541–550, https://doi.org/10.1016/0038-1101(75)90031-3.

[25] Erdoğan, E., Kundakçı, M. 2017. Room temperature current-voltage (IV) characteristics of Ag/InGaN/n-Si Schottky barrier diode. Phys. Conden. Ma. 506: 105–108, https://doi.org/10.1016/ j.physb.2016.11.005.